

---

# Princeton Plasma Physics Laboratory

---

PPPL-

PPPL-



Prepared for the U.S. Department of Energy under Contract DE-AC02-09CH11466.

# Princeton Plasma Physics Laboratory

## Report Disclaimers

---

### Full Legal Disclaimer

This report was prepared as an account of work sponsored by an agency of the United States Government. Neither the United States Government nor any agency thereof, nor any of their employees, nor any of their contractors, subcontractors or their employees, makes any warranty, express or implied, or assumes any legal liability or responsibility for the accuracy, completeness, or any third party's use or the results of such use of any information, apparatus, product, or process disclosed, or represents that its use would not infringe privately owned rights. Reference herein to any specific commercial product, process, or service by trade name, trademark, manufacturer, or otherwise, does not necessarily constitute or imply its endorsement, recommendation, or favoring by the United States Government or any agency thereof or its contractors or subcontractors. The views and opinions of authors expressed herein do not necessarily state or reflect those of the United States Government or any agency thereof.

### Trademark Disclaimer

Reference herein to any specific commercial product, process, or service by trade name, trademark, manufacturer, or otherwise, does not necessarily constitute or imply its endorsement, recommendation, or favoring by the United States Government or any agency thereof or its contractors or subcontractors.

---

## PPPL Report Availability

### Princeton Plasma Physics Laboratory:

<http://www.pppl.gov/techreports.cfm>

### Office of Scientific and Technical Information (OSTI):

<http://www.osti.gov/bridge>

---

### Related Links:

[U.S. Department of Energy](#)

[Office of Scientific and Technical Information](#)

[Fusion Links](#)

Effects of enhanced cathode electron emission on Hall thruster operation

Y. Raitses,<sup>1</sup> A. Smirnov<sup>2</sup> and N. J. Fisch

Princeton Plasma Physics Laboratory

Princeton, NJ 08543

ABSTRACT

Interesting discharge phenomena are observed that have to do with the interaction between the magnetized Hall thruster plasma and the neutralizing cathode. The steady-state parameters of a highly ionized thruster discharge are strongly influenced by the electron supply from the cathode. The enhancement of the cathode electron emission above its self-sustained level affects the discharge current and leads to a dramatic reduction of the plasma divergence and a suppression of large amplitude, low frequency discharge current oscillations usually related to an ionization instability. These effects correlate strongly with the reduction of the voltage drop in the region with the fringing magnetic field between the thruster channel and the cathode. The measured changes of the plasma properties suggest that the electron emission affects the electron cross-field transport in the thruster discharge. These trends are generalized for Hall thrusters of various configurations.

<sup>1</sup> E-mail: [yraitses@pppl.gov](mailto:yraitses@pppl.gov)

<sup>2</sup> Presently with Tri Alpha Energy Inc., Foothill Ranch, CA 92610 USA

## I. INTRODUCTION

The Hall thruster (HT)<sup>1</sup> generates thrust due to the electrostatic acceleration of ions in a quasineutral plasma with crossed electric and magnetic fields. A low pressure cross-field discharge is sustained in the ceramic channel between the anode and a thermionic hollow cathode, which also serves as the ion beam neutralizer. The working gas flow is usually highly ionized ( $> 80\%$ ) in the thruster discharge inside the channel. An additional smaller gas flow through the cathode is ionized inside the hollow emitter. The ionic current flowing to the emitter provides enough heating to keep it at the emission temperature. Gas discharges with such self-heated thermionic cathodes are commonly referred to as self-sustained.<sup>2</sup> The typical parameters of the thruster plasma are as follows: density  $\sim 10^{12} \text{ cm}^{-3}$ ; electron temperature  $\sim 20\text{-}50 \text{ eV}$ ; ion energy  $\leq 10^3 \text{ eV}$ ; electric field  $\sim 10^2 \text{ V/cm}$ ; and magnetic field  $\sim 10^2 \text{ Gauss}$ .

Currently proposed theories of HT's predict that the thruster discharge current is determined by the ionization of the working gas, wall losses, and the electron conductivity across the magnetic field.<sup>1,3-9</sup> These parametric dependencies suggest that at a given discharge voltage, when the gas flow is fully ionized, the discharge current is limited by the magnetic field. However, recent experiments demonstrate a fundamentally different situation when the self-sustained magnetized thruster discharge is also limited by the electron source.<sup>10-12</sup> By increasing the cathode electron emission, the discharge current is increased above its normal value required for self-sustaining the steady-state discharge (at given gas flow, magnetic field and discharge voltage).<sup>10</sup> Only when the discharge current saturates with the electron emission, the

thruster discharge, which is non-self-sustained now, becomes limited just magnetically. The changes of the discharge current are accompanied by the changes in the distributions of the thruster plasma parameters.<sup>11</sup>

The above results were demonstrated for low power (100-200 W) cylindrical Hall thrusters (CHT) with a hollow cathode<sup>10,11</sup> and a hot filament cathode.<sup>12</sup> With the hollow cathode, the electron supply was increased by running an auxiliary discharge, powered from a separate power supply, between the cathode emitter and an intermediate electrode, the so-called cathode keeper. The keeper current was several times larger than the discharge current, which is an unusual regime of the hollow cathode operation. In the filament cathode case, thermionic electron emission was controlled by varying the temperature of the filament wire.<sup>12</sup> The filament heating was provided by an external power supply.

The sensitivity of the thruster operation and performance to boundary conditions at the cathode side of the thruster discharge and the cathode operating parameters was reported in several experimental studies of different HTs,<sup>13-15</sup> including high performance medium power (1-8 kW) conventional annular thrusters (10-15 cm outer diameter (OD) of the channel filled with the plasma). However, the non-self-sustained operation of smaller, low power Hall thrusters with the enhanced electron emission makes a more dramatic impact on the thruster performance.<sup>10</sup> For the 100 W (3 cm OD) CHT, the enhancement of the electron supply with a keeper current for the hollow cathode, and with a wire heating for the filament cathode, led to up to 30% narrowing of the plasma plume and nearly twofold increase in the fraction

of high-energy ions. These improvements in the production and focusing of energetic ions resulted in up to 20% increase of the thrust.

The enhancement of the cathode electron emission also leads to the suppression of the large amplitude low frequency discharge current oscillations, which are ubiquitous in the conventional Hall thruster discharge.<sup>16-18</sup> Theories attribute these oscillations to various ionization mechanisms<sup>1,7,19,20</sup> and to a Buneman-type current instability.<sup>21</sup> The present study points to the correlation between these current oscillations and the negative differential resistance of the plasma in various regions of the thruster discharge.

In this paper, we generalize the effects of the cathode electron emission to low power Hall thrusters of various geometries, including annular and cylindrical, and various magnetic field topologies, including mirror- and cusp-types, and the conventional configuration with a strong radial component of the applied magnetic field. An important practical implication of this work is that it demonstrates that in the normal self-sustained regime of the Hall thruster operation, the supply of electrons from the cathode, the ionization of the working gas, and the ion acceleration can be strongly coupled and, therefore, are not easy to control and optimize. Three major issues, which are difficult to treat because of such a coupling, are large plasma plume divergence, enhanced electron cross-field transport, and large amplitude discharge current oscillations. Controlling the cathode electron emission independently of the main thruster discharge is shown to affect the electron cross-field transport, reduce the beam divergence, and suppress the low frequency discharge current oscillations.

The thruster configurations and the experimental setup are described in Sec. II and Sec. III, respectively. The results of the measurements are presented in Sec. III. The main conclusions and some practical implications are summarized in Sec. IV.

## II. THRUSTER CONFIGURATIONS

The CHT<sup>22</sup> (Fig. 1) features a combination of the gridless Kaufman ion source<sup>23</sup> (end-Hall thruster) and the conventional annular HT with ceramic channel walls (stationary plasma thruster or SPT).<sup>1</sup> The detailed comparison of these thrusters is presented in Ref. 24. The CHT has a lower surface-to-volume ratio than the SPT and, thus, seems to be more suitable for miniaturization, which is required for low power space applications. The principle of operation of the CHT is in many ways similar to that of the SPT, i.e., it is based on a closed  $E \times B$  electron drift in a quasineutral plasma. However, the CHT differs fundamentally from the SPT in that electrons in the cylindrical design provide charge neutralization of ions not by not moving axially, but being trapped axially in a hybrid magneto-electrostatic trap.<sup>25</sup> A similar axial trap for electrons should exist in the mirror-type magnetic configuration of the end-Hall thruster with conductive channel walls. However, the weaker insulating properties of the magnetized plasma in this thruster limit operation to relatively lower discharge voltages ( $\sim 100$  V) than in the CHT and SPT.

In the described experiments, the 2.6 cm and 3 cm OD laboratory Hall thrusters were used. Both thrusters have similar flexible and modular design. Fig. 2 shows the schematic of the 2.6 cm CHT, which has two electromagnet coils, with the

superimposed magnetic field. The main gas flow is supplied through the anode, which serves also as a gas-distributor. The thruster channel can be with or without a short annular part (Fig. 2a and b, respectively), which serves to maintain higher ionization.<sup>22</sup> However, the presence of the annular part has a small effect on the overall CHT performance, while its absence simplifies the thruster design.<sup>26,27</sup>

By varying the relative polarity of the currents in the thruster electromagnets, two magnetic field configurations can be generated: “direct” (or enhanced mirror) with an enhanced axial component of the magnetic field (Fig. 2a) and “cusp” with an enhanced radial component (Figs. 2b) in the cylindrical part of the channel. The results of the comprehensive studies of the CHT with cusp-type and mirror-type magnetic field configurations were reported elsewhere.<sup>22,25,28</sup> For the miniaturized low power CHT, the mirror-type magnetic field configuration has a higher efficiency.<sup>28</sup>

By extending the central pole of the magnetic core and the central ceramic piece up to the exit plane of the channel, the 2.6 cm CHT can be converted to the conventional annular thruster (Fig. 2c). The outer and the inner diameters of the annular boron nitride channel are 2.6 cm and 1.4 cm, respectively. In previous studies,<sup>29</sup> both annular and cylindrical configurations of the 2.6 cm thruster demonstrated comparable performance.

### III EXPERIMENTAL SETUP

The thrusters were operated in the large PPPL Hall Thruster facility. The thrusters, facility, and diagnostics used in these experiments are described elsewhere.<sup>25</sup>

In all experiments, the working gas was xenon. The operating pressure in the 28 m<sup>3</sup> vacuum vessel equipped with cryopumps did not exceed 3  $\mu$ torr. A commercial thermionic hollow cathode<sup>30</sup> was used as the cathode-neutralizer. This cathode consists of a hollow tube with a barium-impregnated porous tungsten emitter, enclosed by an intermediate keeper electrode. The cathode gas (xenon) flow rate was maintained constant and equal to 2 sccm. The thruster, cathode, and the thruster power supplies were floating with respect to the ground. No passive or active filters were used in the thruster or cathode electric circuitries. For both annular and cylindrical thruster configurations the cathode position with respect to the thruster was similar to that used in the previously reported experiments.<sup>11,25,27-29</sup> The cathode keeper electrode was used to initiate the main discharge between the cathode and the thruster anode. In addition, the keeper electrode was also used to maintain the auxiliary cathode discharge in the non-self-sustained operation.<sup>10,11,27</sup>

The plasma diagnostics used in these experiments, including the planar plume probe with a guarding ring, retarding potential analyzers for measurements of ion energy distribution function (IEDF), and the set of miniaturized planar Langmuir probes for measurements inside the channel of the CHT, are described elsewhere.<sup>10,12,31</sup> For the annular Hall thruster, a stationary floating emissive probe was used to determine the plasma potential at the channel exit. The plasma potential was deduced assuming space-charge limited emission from the probe filament.<sup>32</sup> Moreover, a movable cylindrical Langmuir probe was used to characterize plasma properties in the near-field plasma plume.

The ion plume diagnostics were placed on rotating arms to measure the angular distribution of the ion current and IEDF in the far plume at the distance of 70 cm from the thrusters. The plume angle, which is customary defined as the angle that contains 90% of the total ion current, was estimated from the measured angular ion flux distribution. The ionization efficiency (or propellant utilization) of the discharge is characterized by the ratio of the total ion current to the mass flow rate of the working gas in units of current. The ratio of the total ion current to the discharge current is used to characterize the insulating properties of the magnetized thruster plasma.

### III. EXPERIMENTAL RESULTS AND DISCUSSIONS

#### **A. Thruster parameters and cathode operation**

Experimental results are presented for the following operating parameters of the annular and cylindrical Hall thruster configurations: the discharge voltage of 250 V and the anode gas flow rates of 3.4 sccm and 4 sccm, respectively. The thrusters were operated with and without the cathode-keeper discharge. Fig. 3 shows illustrative curves of the V-I characteristic of the cathode-keeper discharge measured with and without the thruster discharge. This shape of the V-I characteristic without the thruster discharge is typical for hollow cathodes used for ion and Hall thrusters.<sup>33</sup> The keeper discharge was usually in a stable current-limited mode when it operated on the horizontal part of its V-I characteristic. For the non-self-sustained operation, the keeper current was in the range of 2-3 A. For different cathodes used in these

experiments, the keeper voltage at this current level could be different, but usually within the range of 10-15 V (Fig. 3 and Ref. 24).

## **B. Plasma plume narrowing**

For all three thruster configurations shown in Fig. 2, the cathode electron emission has a striking effect on the angular ion current distribution (Fig. 4). With all thruster parameters the same, the plume divergence of the generated plasma flow decreases dramatically as the cathode keeper current is increased (Fig. 5). A similarly strong plume narrowing was measured for the CHT with and without a short annular part.<sup>27</sup> Apparently, the changes of the thruster configuration from the CHT to the conventional annular HT, of the magnetic field topology and thruster operating parameters, including the gas flow rate and the discharge voltage (e.g. for annular HT in Fig. 4b) do not change the general trends of the cathode effect on the plume angle. A relatively smaller plume narrowing measured for the annular HT may be attributed to the defocusing shape of the magnetic field surfaces in this thruster. The plume narrowing is evident not only from the probe measurements, but also from the observation of the plasma plume with the naked eye (for the annular HT, Fig. 6).

Note that the ion flow in the thruster plume is well charged-neutralized for both normal and non-self-sustained regimes. Plasma measurements in the plume of the annular HT showed that the radial voltage potential drop,  $\Delta\phi$ , in the plume is varied from roughly 10 V at the distance of 10 cm downstream from the thruster along the thruster symmetry axis to less than a volt in the far-field plume (70 cm from the

thruster). The reduction of the potential drop with the electron emission did not exceed a couple of volts at the distance of 10 cm from the thruster and much less at larger distances. For an ion accelerated to  $\varepsilon_{\text{ion}} = 250$  eV, the maximum change of the divergence angle due to this reduction,  $(\Delta\phi_n^{0.5} - \Delta\phi_{\text{ns}}^{0.5})/\varepsilon_{\text{ion}}^{0.5}$ , should be around  $1^\circ$ , while the measured plume narrowing is  $7\text{-}8^\circ$  for a half plume angle.

The narrowing of the plume is accompanied by an increase of the average energy and the number of energetic ions at the thruster symmetry axis (Fig. 7 for the annular HT and Refs. 10 and 27 for the CHT). At the same time, the number of high-energy ions flying at large angles to the axis decreases. The peak ion energy shifts towards higher energies with the increasing keeper current. For the annular HT, this shift is slightly larger than 5 eV and 10 eV for the centerline and the larger angles, respectively (Fig. 7), while for the CHT, the peak ion energy was shifted 20-30 eV with the keeper current.<sup>10,27</sup> Such modifications of the IEDF means that, in the non-self-sustained regime, ions are born at higher potential.<sup>12</sup> Integrated over the azimuthal angle, these changes in the distribution of the ion current density and average ion energy lead to the increase of the thrust.<sup>25</sup> This result is in an agreement with the thrust measurements (for the CHT, up to a 20% thrust increase).<sup>10,27</sup>

### **C. Transition from electron source-limited to magnetically-limited discharge**

Both annular and cylindrical HTs produce highly ionized plasma flow.<sup>29</sup> It seems therefore surprising that the increase of the cathode electron emission can still cause changes of the discharge current and parameters of the plasma flow (Fig. 5).<sup>11</sup>

What is also interesting is that the discharge current,  $I_d$ , the ion current  $I_{ion}$ , and the electron cross-field current,  $I_{e\perp} \approx I_d - I_{ion}$ , (Fig 5d) in the cusp and direct magnetic configurations of the CHT exhibit different behaviors as the cathode electron emission increases. Namely, the discharge current initially grows in the direct configuration and decreases in the cusp one, but saturates starting the keeper current  $\sim 2 - 2.5$  A (Fig. 5a). The same threshold value of the keeper current was obtained for both magnetic field configurations and various electromagnet coil currents (i.e. various magnitudes of the magnetic field). In both the self-sustained and non self-sustained regimes, the discharge current tends to increase when the magnetic field is reduced. Thus, at sufficiently large values of the keeper current, the thruster discharge is indeed magnetically limited<sup>11</sup> and not controlled by the electron emission.

Recent time-of-flight measurements<sup>27</sup> in the 3cm CHT of the direct configuration confirmed the presence of multicharged xenon ions in the thruster plume, which explains large values ( $> 1$ ) of the propellant utilization in Fig. 5c. For example, at  $40^\circ$  from the thruster centerline, the partial fluxes of doubly and triply charged ions increased from roughly 10% and 2% of the total ion flux at no keeper current to, roughly, 20% and 30%, respectively, at the keeper current of 2-3A.<sup>27</sup> The formation of multiply charged ions in the CHT is believed to be due to the increased residence time of slow ions born in the near axis region of the cylindrical channel.<sup>25</sup> These ions are trapped in the radial direction by an ambipolar potential hill that is predicted to appear at the thruster axis due to ion beam focusing. This mechanism is indirectly supported by the experimental data of Ref. 27, which showed that the fraction of multiply charged ions increases with decreasing energy-to-charge ratio. Apparently, the

increase of the production of these ions with the cathode electron emission leads to the increase of the propellant utilization in the direct configuration of the CHT (Fig. 5c). Finally, for the annular HT, the discharge current increases (Fig. 8) mainly due to the increase of the electron cross-field current with the electron emission.

To summarize, these results imply that with all thruster parameters the same, there can be more than one thruster steady-state, which for a given cathode placement with the respect to the magnetic field, depends on the cathode electron emission or, more generally, on the boundary conditions imposed by the cathode. This dependence is strong while the discharge is the electron source-limited. Once it has evolved to the magnetically-limited mode, the discharge current is no longer affected by the increase of the electron emission. It is this particular case that is considered by a majority of the existing Hall thruster models.

The cathode position relative to the magnetic field can also affect the discharge current and the plasma plume. These effects were observed for high performance conventional HTs equipped with thermionic hollow cathodes<sup>13-15</sup> and for a low power CHT thruster operated with a thermionic filament cathode.<sup>12</sup> The discharge current and performance (in particular, the plume angle and utilization efficiencies) improved gradually with the increasing temperature of the filament wire, until reaching the saturation. The saturated values of these parameters were sensitive to the cathode placement. Optimization of the cathode position at a given filament temperature led to the plume narrowing. However, the magnitude of this effect was less than that due to the increase of the electron emission.<sup>12</sup> It is likely that the cathode placement and the electron emission affect the boundary conditions at the cathode by different means:

injection of electrons into the magnetized plasma and the supply of electrons (or electron density), respectively.

#### **D. Discharge structures and plasma properties**

The variations of the thruster steady-state with the cathode electron emission are reflected in changes of the distributions of the plasma parameters.<sup>11</sup> For the annular HT, Fig. 8 shows the dependences of plasma potential at the channel exit and the discharge current on the cathode keeper current. The distributions of the plasma potential and the electron temperature measured in the CHT channel and in the near-field plume are shown in Fig. 9.

For all three thruster configurations, the changes of the plasma potential distribution with the keeper current correlate with the attained plume narrowing. For each thruster configuration operating with the non-self-sustained discharge, the voltage drop outside the channel is 2-3 times smaller than that for the self-sustained discharge. Because the discharge voltage is constant, the larger voltage drop is developed inside the thruster channel. In addition, the acceleration region is getting narrower in the CHT channel, especially for the direct configuration (Fig. 9a).

The magnetic field inside the thruster channel, especially for the annular HT, has a stronger radial component than that outside the channel in the fringing magnetic field (Fig. 2). Therefore, the ions might have a larger axial velocity component inside the channel and spend less time in the defocusing fringing magnetic field outside the channel.<sup>34</sup> This might explain the plume narrowing effect with the increase of the

voltage drop inside the thruster channel. Indeed, a rough estimate of the ion trajectories in the annular thruster suggests that the reduction of the outside potential drop from 70 V to 40 V might explain the observed plume narrowing ( $\Delta\phi_s^{0.5}/\epsilon_{is}^{0.5} - \Delta\phi_{ns}^{0.5}/\epsilon_{ins}^{0.5} \sim 10^\circ$ ).

Interestingly, a quantitatively similar plume narrowing was obtained for the larger HTs by controlling the electric-field profile through the use of segmented electrodes.<sup>35</sup> This plume narrowing was also attributed to the increase of the voltage drop inside the thruster channel. This increase was explained by the reduction of the electron cross-field transport associated with the wall-induced mechanism (near-wall conductivity). The near-wall conductivity is predicted to be strong when the secondary electron emission (SEE) from the channel walls is strong.<sup>1,3,6</sup> Floating and cathode biased segmented electrodes placed in the thruster channel have much smaller SEE than the ceramic walls of the conventional HT. In the present experiments, the same ceramic wall material is used for all thruster configurations and operating conditions. Because the SEE is a strong function of the energy of primary electrons, a contribution of the near-wall conductivity, if it takes place in the miniaturized thrusters, might still vary with the electron emission due to differences in the electron temperature (Fig. 9b).

It should be noted that in the described experiments, the electron temperature was deduced from the probe measurements under the assumption of the Maxwellian EEDF.<sup>31</sup> For a collisionless plasma of the annular HT and CHT thrusters, the electron energy distribution function (EEDF) is predicted to depart from Maxwellian.<sup>36,37</sup> Presumably, the measured reduction of the electron temperature with the electron emission reflects the reduction of the mean electron energy. This reduction may be a

signature of the electron kinetic effects, which are predicted to occur in the magnetic mirror and are associated with the cooling of  $E \times B$  rotating particles moving along equipotential magnetic field surface.<sup>38</sup>

In Ref. 11, the differences in the plasma potential distributions observed with and without the keeper current were analyzed for the direct configuration of the CHT. The measured plasma and plume parameters were used together with the generalized Ohm's law in the direction across the magnetic field. Previous studies of the CHT suggested that the electron cross-field transport in this thruster is anomalous and mainly by fluctuation-enhanced mechanism.<sup>25,37</sup> Therefore, Ref. 11 used the Bohm-like scaling for the anomalous collision frequency,  $\nu_B = \kappa_B \omega_c / 16$ ,<sup>25</sup> which determines the electron cross-field mobility,  $\mu_{\perp} \propto \nu_B / \omega_c^2$ . Here,  $\kappa_B$  is the dimensionless parameter and  $\omega_c$  is the electron gyrofrequency. The results of this analysis showed that the anomalous collision frequency is almost twice times smaller for the direct CHT operating with the non-self-sustained discharge in the magnetically-limited mode. The same analysis can be applied for the cusp configuration of the CHT. The average values of the electron current and plasma density (not shown in this paper) in the cylindrical part of the channel differ slightly for the self-sustained and non-self-sustained discharges, while the electric field is almost twice greater in the latter case. Therefore, the anomalous collision frequency parameter obtained from the Ohm law,  $\kappa_B \sim I_e B / (N_e E A)$ , where  $B$  is the magnetic field,  $N_e$  is the plasma density,  $E$  is the electric field, is likely smaller for the non-self-sustained discharge. Here, for the sake of simplicity, we neglected pressure term, which is smaller than the electric field term inside the channel, and assumed uniform distribution of the electron cross-field current

across the channel with the cross-sectional area  $A$ .<sup>11</sup> Using the measured profiles of the plasma properties in the self-sustained and non-self-sustained discharges, the ratio of the anomalous collision frequency parameters for the cusp configuration is:

$$\frac{\kappa_{B\_s}}{\kappa_{B\_ns}} \propto \frac{J_{e\perp\_s}}{J_{e\perp\_ns}} \times \frac{N_{e\_ns}}{N_{e\_s}} \times \frac{E_{ns}}{E_s} \approx 2,$$

where  $s$  and  $ns$  are the indexes standing for self-sustained and non-self-sustained discharges, respectively. This ratio is larger than the change in the average magnetic field in the acceleration region of the CHTs with the self-sustained and non-self-sustained discharges. Thus, the electron cross-field mobility apparently becomes smaller with the cathode electron emission. This observation implies that in spite of the differences in the behavior of the discharge parameters with the electron emission, the general trend for both CHT configurations is that the insulating properties of the magnetized thruster plasma are stronger when the discharge current is not limited by the supply of electrons from the cathode. The modification of the distribution of the electron cross-field mobility with the cathode electron emission is likely responsible for the observed restructuring of the thruster discharge at different steady states.

The results of the above analysis are applicable if the cathode electron emission does not alter the distribution of the electron cross-field current across the channel ( $A \sim \text{constant}$ ). In principle, following Ohm's law, the existence of the stronger electric field in the non-self-sustained discharge could be obtained if the electron current density across the channel were locally increased without alteration of the total electron cross-field current. However, in this case, the enhanced Joule heating would

lead to a higher electron temperature, whereas what is observed is the cooling of electrons observed for the non-self-sustained discharge (Fig. 9b).

### **E. Discharge current oscillations**

A remarkable feature of the non-self-sustained thruster discharge is that in the magnetically-limited mode, it is free of large amplitude low frequency discharge current oscillations (Figs. 10 and 11). These oscillations with the frequency of 10-30 kHz are usually observed in the conventional Hall thrusters.<sup>16-18</sup> They can cause a mismatch between the power supply and the thruster discharge, induce a source of electromagnetic interference, and contribute to the plume divergence.<sup>7,20</sup> For the cylindrical Hall thrusters, the large amplitude discharge current oscillations are not always featured,<sup>22,26,29</sup> but when they appear, their characteristic frequency is typically lower ( $\sim 10$  kHz on Fig. 11 and Refs. 22 and 26) than measured for the annular HT ( $\sim 20$  kHz on Fig. 10).

Physical mechanisms responsible for generating low frequency oscillations in the Hall thrusters are not well understood. Several numerical studies reproduced and provided different interpretations of these oscillations. The possible explanations include 1) motion of the ionization front<sup>7</sup> due to the periodic depletion of neutral atoms in the ionization region with the characteristic frequency  $\omega \sim 2\pi (v_a/L)$ , where  $v_a \sim 10^4$  cm/sec is the velocity of atoms and  $L \sim 1$  cm is the characteristic length of the region, 2) an ionization predator-prey cycle<sup>19,20,39</sup> with the characteristic frequency  $\omega = (v_{\text{ion}}v_a/L^2)^{0.5}$ , where  $v_{\text{ion}} \sim 10^6$  cm/sec is the ion velocity, and 3) the Buneman-type

current instability,<sup>21</sup> which is due to the coupling between the ion current and the self-consistent electric field. Finally, it is also known that the azimuthal waves, which can become unstable when  $\partial(B/N)/\partial z < 0$ , where  $z$  is the axial coordinate, give rise to low frequency oscillations in the thruster discharge.<sup>1</sup> This particular mechanism may be relevant to the miniaturized cylindrical Hall thruster, where the magnetic field has the maximum at the anode. Active and passive filters in the external electric circuitry of the discharge, and specially designed magnetic field profiles were proposed and used in order to mitigate these oscillations in the thruster.<sup>1,21,39</sup> Apparently, the increase of the cathode electron emission can suppress these oscillations without circuit filters or the change of the magnetic design (Figs. 10 and 11).

In a typical Hall thruster, the discharge current is almost unchanged with the discharge voltage. However, as it is shown in this study, at the given discharge voltage, the discharge current can be regulated by the cathode electron emission. For the miniaturized annular HT and direct CHT configurations, the enhancement of the electron emission correlates with the increase of the discharge current and the reduction of the voltage potential drop in the region of the fringe magnetic field (Fig. 8 for the annular HT and Figs. 5a and 9a for the CHT). For the cusp configuration, the discharge current reduces with the electron emission, while the voltage drop inside the thruster channel increases. Thus, for each thruster configuration, there is a discharge region with a local negative differential resistance,  $dU/dI < 0$ . For the annular HT and direct CHT, this region is located outside the thruster channel, while for the cusp CHT, this region is inside the thruster channel. It is well known that self-sustained discharges and plasma-beam systems with such a voltage-versus-current characteristic

may exhibit relaxation oscillations.<sup>2,40</sup> The suppression of the current oscillations with the cathode electron emission coincides with the saturation of the potential drops inside and outside of the thruster channel i.e., with  $dU/dI \sim 0$ .

The existence of the local negative differential resistance in the self-sustained thruster discharge implies that the current oscillations should be accompanied by the oscillatory behavior of the plasma potential distribution. For example, for the annular HT, the increase of the discharge current should lead to the increase of the voltage drop inside the channel. If, as predicted by numerical simulations,<sup>7</sup> the neutral depletion caused by ionization of the working gas is responsible for the next phase of oscillations when the discharge current reduces, the non-self-sustained regime should also be subjected to this process. Apparently, this is not the case observed in these experiments. Therefore, other physical mechanisms independent of the neutral transport are likely responsible for low frequency oscillations.

Note that, the cathode-keeper discharge also has a downward sloping V-I characteristic with  $dU/dI < 0$  at low keeper currents (Fig. 3). The increase of the cathode heating with the keeper current leads to the flattening of the V-I characteristic ( $dU/dI \sim 0$ ). When the cathode operates together with the main thruster discharge, the saturation of the cathode-keeper voltage occurs at smaller values of the keeper current (Fig. 3). Apparently, this is due to the combined cathode heating by both the thruster and keeper discharges. For all three thruster configurations, the changes of the cathode-keeper voltage with the keeper current up to 3 A are less than a half of the reduction of the voltage drop outside the thruster channel (Figs. 8 and 9a). Moreover, the keeper-cathode voltage drop saturates usually at the keeper current of  $\sim 1$  A, while

the thruster discharge parameters continue changing at larger values of the keeper current (Figs. 3 and 8). These results suggest that if the presence of the discharge region with a negative differential resistance is associated with the low frequency current oscillations, the observed changes of the plasma potential distribution with the cathode electron emission play a major role in their suppression.

#### IV. CONCLUSIONS

The cathode electron emission is shown to have profound effects on the efficient and stable generation of the focused plasma flow in Hall thrusters of various geometries and magnetic field topologies, including cylindrical Hall thrusters with the cusp and mirror magnetic fields and the conventional annular Hall thrusters. Although the detailed physics of these effects is still not fully understood, we summarize below the main observations and their possible explanations.

In the non-self-sustained thruster discharge, the electron emission is controlled independently of the main thruster discharge. Decoupling of the cathode electron emission from the main plasma processes, namely ionization of the working gas and the ion acceleration, leads to a better focusing of the plasma flow, enhances the insulating properties of the magnetized plasma, and suppresses the ubiquitous large amplitude, low frequency discharge oscillations. These improvements are achieved in the limit of a strong electron emission from the cathode, when the thruster discharge current at a given gas flow rate becomes limited just magnetically as opposed to the normal mode, limited also by the electron source.

Plasma measurements suggest that the significant plume narrowing, which is observed for the non-self-sustained discharge in all thruster configurations, is due to a smaller electric field in the region of the defocusing fringe magnetic field. The non-self-sustained discharge is also associated with the changes of the electron anomalous cross-field transport. In particular, the electron cross-field mobility appears to decrease in the region with a strong magnetic field (inside the thruster channel) and increase in the weaker, fringe magnetic field between the cathode and the channel exit. The reduction of the electron transport inside the thruster channel correlates with the electron cooling, which may be a manifestation of the recently predicted electron kinetic effects in  $E \times B$  rotating plasmas characteristic of the mirror and cusp configurations of the cylindrical Hall thruster.

Finally, the non-self-sustained regime of the thruster discharge breaks a chain of plasma processes leading to the large amplitude discharge oscillations. The suppression of these oscillations at a constant discharge voltage correlates with change of the local V-I characteristics of the plasma discharge inside and outside of the thruster channel. For both annular and cylindrical thrusters, this change always involves the reduction of the outside voltage drop with the increase of the cathode electron emission. In this regime, there are no plasma regions with the negative differential resistance, which are normally observed for the self-sustained operation. More work has to be done in order to understand the mechanisms of these oscillations and their suppression observed in these experiments.

## ACKNOWLEDGMENT

The authors wish to thank Dr. Kevin Diamant, Mr. Erik Granstedt and Mr. Jeffrey Parker for their contributions to the experiments and fruitful discussions. The authors also benefited from insightful discussions with Dr. Igor Kaganovich, Dr. Michael Keidar, Dr. Alexander Kapulkin and Dr. Amnon Fruchtman. This work was supported by US DOE under Contract No. AC02-76CH0-3073.

## REFERENCES

1. A. I. Morozov and V. V. Savelyev, in Review of Plasma Physics, edited by B. B. Kadomtsev and V. D. Shafranov. (Consultants Bureau, New York, 2000) Vol. 21, p. 203.
2. Yu. P. Raizer, Gas Discharge Physics, (Springer-Verlag Berlin Heidelberg New York, 1997) p. 245.
3. M. Keidar, I. Boyd and I. I. Beilis, Phys. Plasmas **8**, 5315 (2001).
4. A. Fruchtman, N. J. Fisch, and Y. Raitses, Phys. Plasmas **8** 1048 (2001)
5. E. Ahedo, J. M. Gallardo, and M. Martínez-Sánchez, Phys. Plasmas **9** 4061 (2002)
6. S. Barral, K. Makowski, Z. Peradzyski, N. Gascon, and M. Dudeck, Phys. Plasmas **10**, 4137 (2003).
7. J. P. Boeuf and L. Garrigues, J. Appl. Phys. **84**, 3541 (1998); J. Bareilles, G. J. M. Hagelaar, L. Garrigues, C. Boniface, J. P. Boeuf, and N. Gascon, Phys. Plasmas **11**, 3035 (2004).
8. L. Garrigues, G. Hagelaar, J. P. Boeuf, Y. Raitses, A. Smirnov, and N. J. Fisch, IEEE Trans. Plasma Sci. **36**, 2034 (2008).
9. E. Fernandez, M. K. Scharfe, C. A. Thomas, N. Gascon, and M. A. Cappelli Phys. Plasmas **15** 012102 (2008).
10. Y. Raitses, A. Smirnov, and N. J. Fisch, Appl. Phys. Lett. **90**, 221502 (2007)
11. A. Smirnov, Y. Raitses, and N. J. Fisch, IEEE Trans. Plasma Sci. **36**, 1998 (2008).
12. E. M. Granstedt, Y. Raitses, and N. J. Fisch, J. Appl. Phys. **104** 103302 (2008).

13. D. L. Tilley, K. H. de Grys, and R. M. Myers, in Proc. *the 35th AIAA Joint Propulsion Conference*, July 1999, Los Angeles, CA (American Institute of Aeronautics and Astronautics, Reston, VA 1999) AIAA paper 99-2865.
14. R. R. Hofer, L. K. Johnson, D. M. Goebel, and R. E. Wirz, IEEE Trans. Plasma Sci. **36**, 2004 (2008).
15. J. D. Sommerville, and L. B. King, in Proc. *the 30th International Electric Propulsion Conference*, 2007, Florence, Italy (Electric Rocket Propulsion Society, Cleveland, OH 2007) IEPC paper 2007-78.
16. A. Bouchoule *et al.*, Plasma Sources Sci. Technol. **10**, 364 (2001).
17. J. Kurzyna, S. Mazouffre, A. Lazurenko, L. Albarède, G. Bonhomme, K. Makowski, M. Dudeck, and Z. Peradzyński, Phys. Plasmas **12**, 123506 (2005).
18. R. B. Lobbia and A. D. Gallimore, in Proc. *the 44<sup>th</sup> AIAA Joint Propulsion Conference*, July 2008. Hartford, CT (American Institute of Aeronautics and Astronautics, Reston, VA 2008) AIAA-2008-4650.
19. J. M. Fife, M. Martinez-Sanchez, and J. Szabo, in Proc. *the 33rd AIAA Joint Propulsion Conference*, 1997, Seattle WA (American Institute of Aeronautics and Astronautics, Reston, VA 1997), AIAA paper 97-3051.
20. S. Barral and E. Ahedo, Phys. Rev. E **79**, 046401 (2009).
21. S. Chable and F. Rogier, Phys. Plasmas **12**, 033504 (2005).
22. Y. Raitses and N.J. Fisch, Phys. Plasmas **8**, 2579 (2001).
23. H. R. Kaufman, R. S. Robinson, and R. I. Seddon, J. Vac. Sci. Technol. **A 5**, 2081 (1987).
24. Y. Raitses, A. Smirnov, and N. J. Fisch, J. Appl. Phys. **104**, 066102 (2008)

25. A. Smirnov, Y. Raitses, and N. J. Fisch, Phys. Plasmas 14, 057106 (2007).
26. A. Shirasaki and H. Tahara, J. Appl. Phys. 101 073307 (2007).
27. K. D. Diamant, J. E. Pollard, Y. Raitses and N. J. Fisch, in Proc. the 44th Joint Propulsion Conference, July 2008, Hartford, CT (American Institute of Aeronautics and Astronautics, Reston, VA 2008) AIAA paper 2008-4998.
28. A. Smirnov, Y. Raitses and N. J. Fisch, IEEE Trans. Plasma Sci. **34**, 132 (2006).
29. A. Smirnov, Y. Raitses, and N. J. Fisch, J. Appl. Phys. **92**, 5673 (2002).
30. Heatwave Labs plasma electron source HWPES-250 (www.cathode.com)
31. A. Smirnov, Y. Raitses and N. J. Fisch, J. Appl. Phys. **95**, 2283 (2004).
32. Y. Raitses, D. Staack, A. Smirnov, and N. J. Fisch, Phys. Plasmas **12**, 073507 (2005).
33. D. Goebel, R. Watkins, K. Jameson, Propul. Power **23**, 552 (2007).
34. A. Fruchtman and A. Cohen-Zur, Appl. Phys. Lett. **89**, 111501 (2006).
35. Y. Raitses, M. Keidar, D. Staack and N.J. Fisch, J. Appl. Phys. **92** 4906 (2002).
36. I. Kaganovich, Y. Raitses, D. Sydorenko and A. Smolyakov, Phys. Plasmas **14**, 057104 (2007).
37. A. Smirnov, Y. Raitses, and N. J. Fisch, Phys. Plasmas **11**, 4922 (2004).
38. N. J. Fisch, A. Fetterman, Y. Raitses, A. Fruchtman, and J. M. Rax, J. M., “*Kinetic Mechanisms of Plume Narrowing in a Cylindrical Hall Thruster*” presented at the 44th Joint Propulsion Conference (Hartford, CT, 2008).
39. S. Barral, J. Miedzik, and E. Ahedo, in Proc. *the 44<sup>th</sup> Joint Propulsion Conference*, July 2008, Hartford, CT, (American Institute of Aeronautics and Astronautics, Reston, VA 2008) AIAA paper 2008-4632.

40. V. L. Granovsky, Electric Current in Gas (Steady Current), (Nauka, Moscow, 1971) p.379 [in Russian].

## List of figures

Fig. 1. The cylindrical Hall thruster (CHT: a) schematic and the principle of operation; b) the 2.6 cm laboratory CHT.

Fig. 2. The 2.6 cm thruster in three configurations used in the experiments, and superimposed magnetic field lines: a) CHT with a direct (mirror-type) magnetic field, b) CHT with a cusp magnetic field and with a short annular part of the channel, c) the annular HT.

Fig. 3 The voltage versus current characteristic of the auxiliary cathode-keeper discharge used to maintain the non-self-sustained operation of the Hall thrusters. The characteristic measured at the cathode xenon gas flow rate of 2 sccm, with and without the main thruster discharge. The former was obtained while the CHT was operated in the direct configuration.

Fig. 4. Plume narrowing effect of the cathode electron emission for the CHT thruster with direct and cusp magnetic field configurations at the discharge voltage of 250 V and xenon gas flow rate of 4 sccm. (a) and for the annular HT at different discharge voltages and the flow rate of 3.4 sccm (b). The ion angular current distribution measured in the far-field plume (70 cm from the thruster) by the planar probe with a guarding sleeve.

Fig. 5. The effect of the auxiliary discharge between the cathode emitter and the cathode keeper electrode on the discharge current (a), plasma plume (b), propellant utilization (c) and the electron cross-field current (d). The thruster operating conditions: the discharge voltage of 250 V and the xenon flow rate of 4 sccm. In each thruster case, the magnetic field is unchanged.

Fig. 6. Plasma plume from the annular Hall thruster in the self-sustained and non-self-sustained regimes. The emissive probe is used to measure the plasma potential at the channel exit. A movable Langmuir probe is used to measure plasma properties in the near-field plume.

Fig. 7. Ion energy distribution function measured for the annular thruster in the far-field plume (70 cm from the thruster) at different angular positions of the retarding potential analyze: a) centerline and b) 30° and 60° with the respect to the centerline. In both self-sustained and non-self-sustained regimes the thruster was operated with the same operating parameters (250V and 3.4 sccm) and the same magnetic field.

Fig. 8. Results of measurements in the annular HT. The effect of the cathode electron emission (keeper current) on the discharge current and the plasma potential (with respect to the cathode) at the channel exit.

Fig. 9. Results of the plasma probe measurement in the CHT for the direct and cusp magnetic field configurations. The thruster was operated in the self-sustained (keeper current = 0 A) and non-self-sustained (keeper current = 2.5 A) regimes at the discharge voltage of 250 V and the xenon gas flow rate of 4 sccm. The plasma potential (a) and the electron temperature (b) were deduced using standard procedures for a biased Langmuir probe.<sup>24</sup> The annular part of the channel is  $0 < z \text{ (mm)} < 6$ ; the cylindrical part of the channel is  $6 < z \text{ (mm)} < 22$ .

Fig. 10. The oscilloscope traces of the discharge current oscillations (a) and corresponding frequency spectrum (b) for self-sustained and non-self-sustained regimes of the annular HT.

Fig. 11. Frequency spectrum measured for the self-sustained and non-self-sustained regimes of the CHT in the direct (a) and cusp (b) magnetic field configurations.

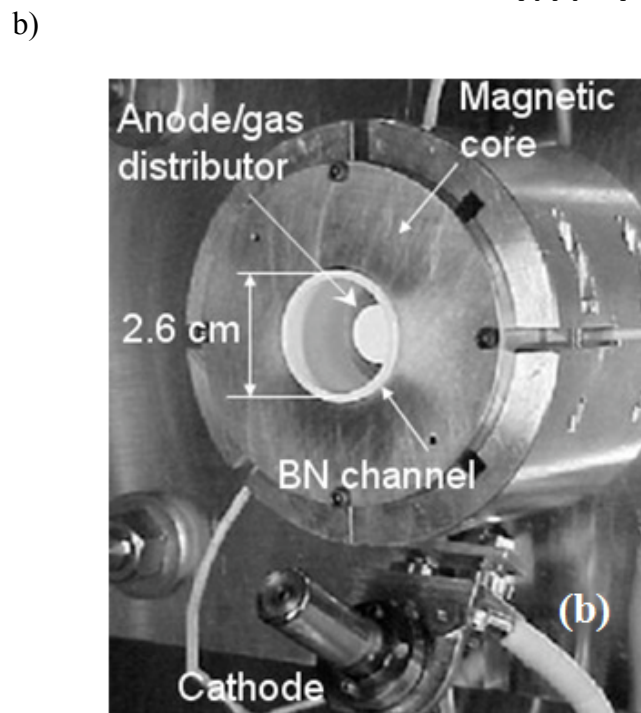
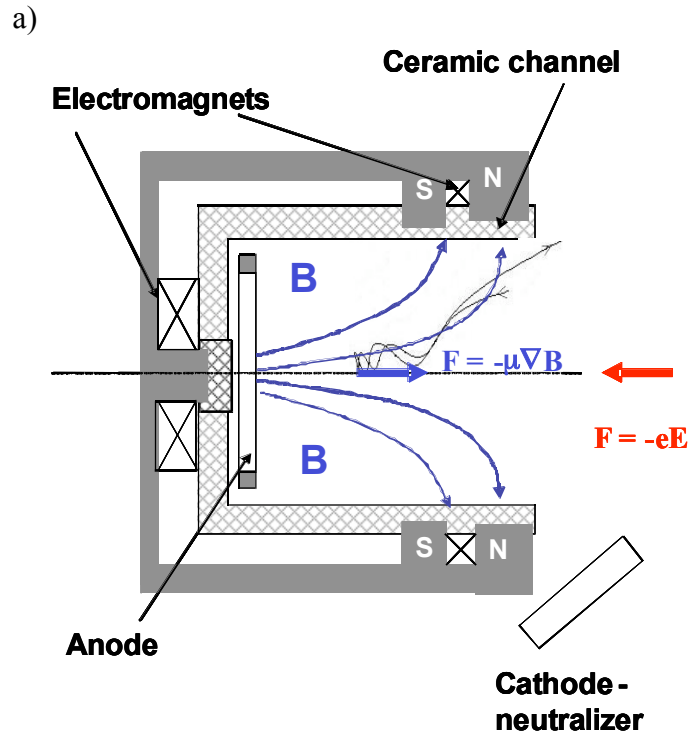
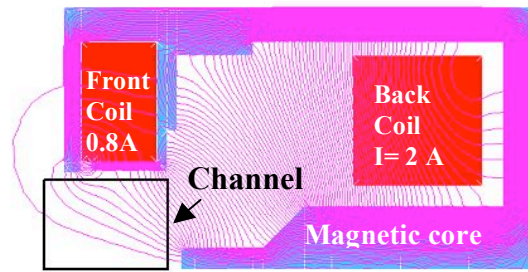
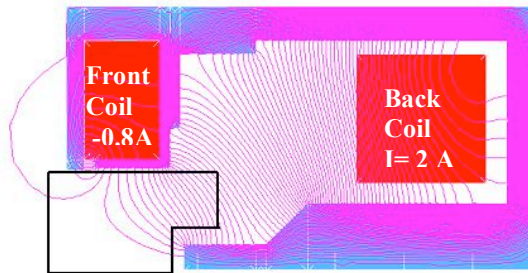


Fig. 1. The cylindrical Hall thruster (CHT: a) schematic and the principle of operation; b) the 2.6 cm laboratory CHT.

a)



b)



c)

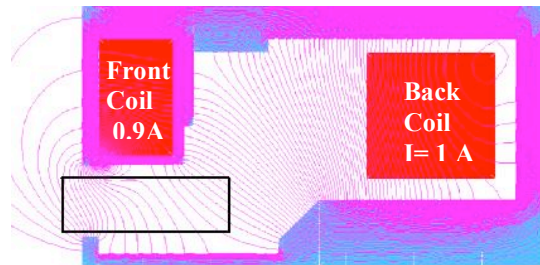


Fig. 2. The 2.6 cm thruster in three configurations used in the experiments, and superimposed magnetic field lines: a) CHT with a direct (mirror-type) magnetic field, b) CHT with a cusp magnetic field and with a short annular part of the channel, c) the annular HT.

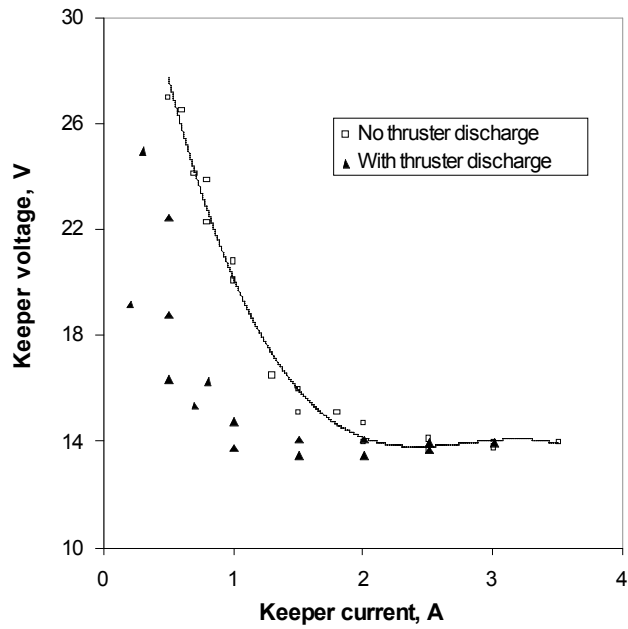
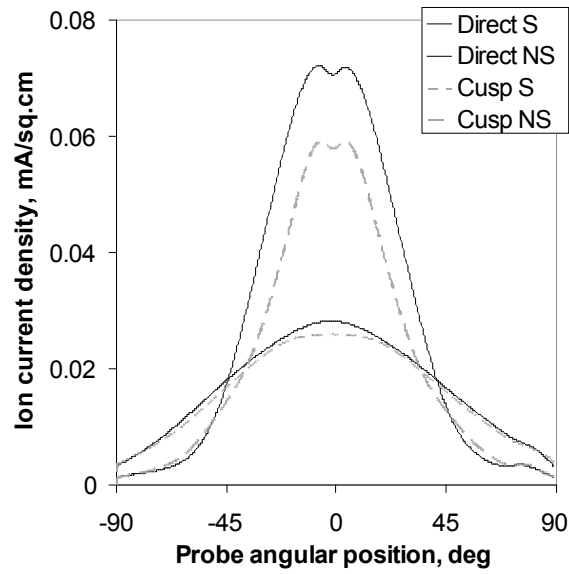


Fig. 3 The voltage versus current characteristic of the auxiliary cathode-keeper discharge used to maintain the non-self-sustained operation of the Hall thrusters. The characteristic was measured at the cathode xenon gas flow rate of 2 sccm, with and without the main thruster discharge. The former was obtained while the CHT was operated in the direct configuration.

a)



b)

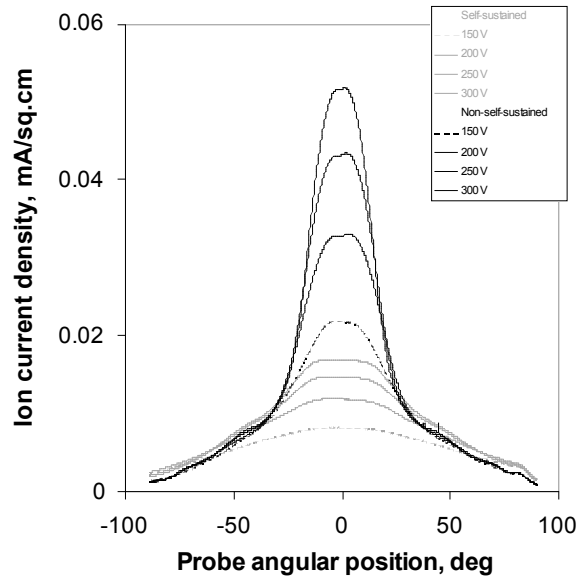


Fig. 4. Plume narrowing effect of the cathode electron emission for the CHT thruster with direct and cusp magnetic field configurations at the discharge voltage of 250 V and xenon gas flow rate of 4 sccm. (a) and for the annular HT at different discharge voltages and the flow rate of 3.4 sccm (b). The ion angular current distribution measured in the far-field plume (70 cm from the thruster) by the planar probe with a guarding sleeve.

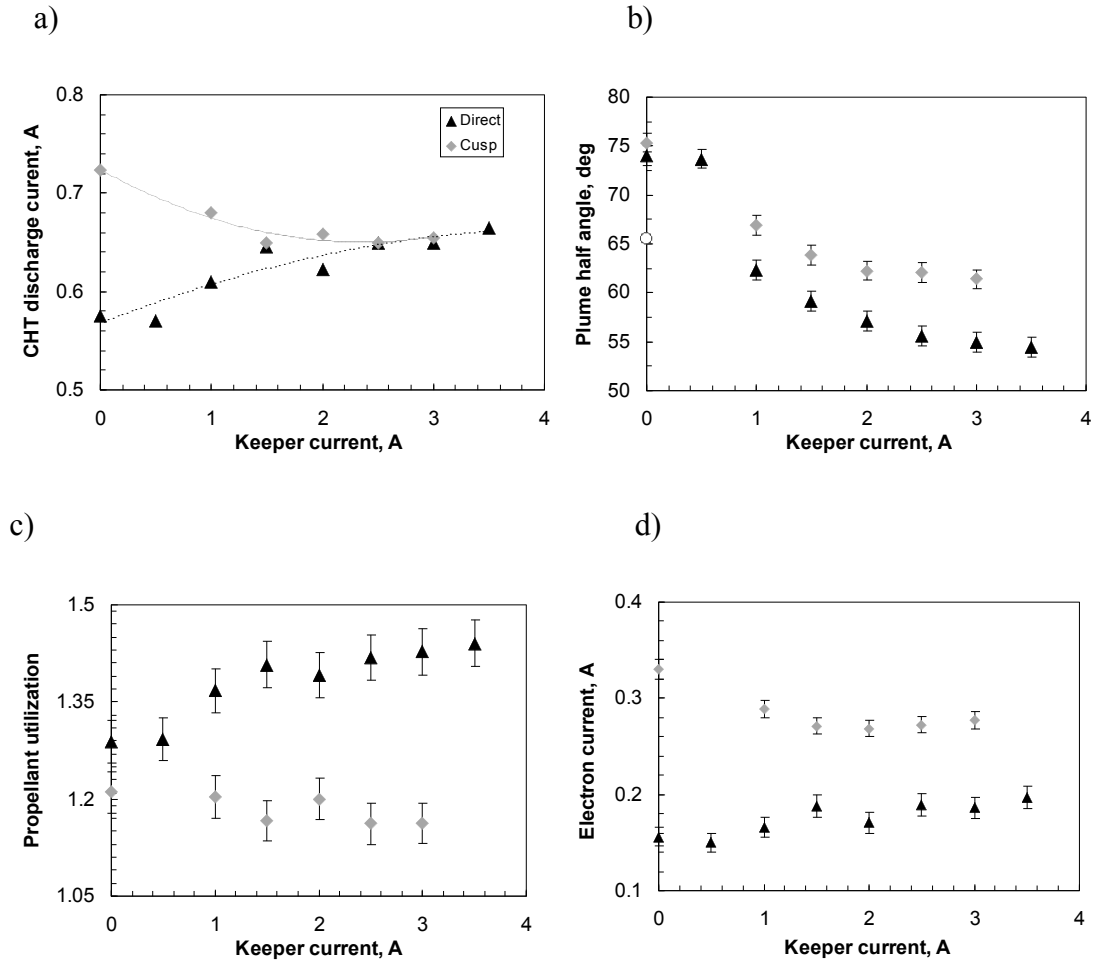


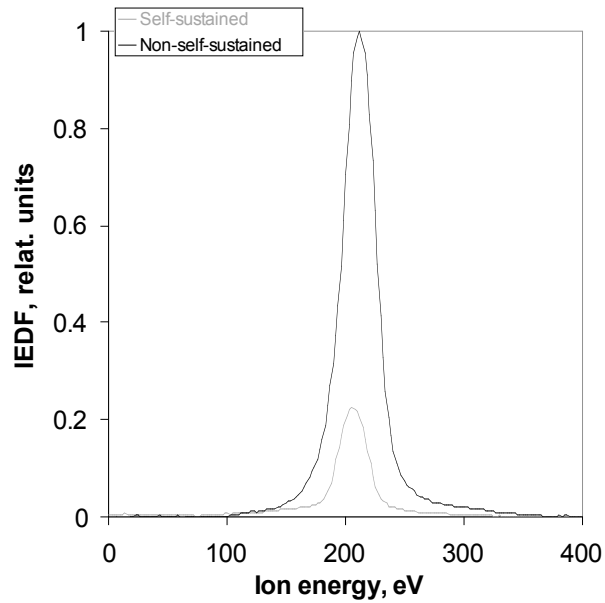
Fig. 5. The effect of the auxiliary discharge between the cathode emitter and the cathode keeper electrode on the discharge current (a), plasma plume (b), propellant utilization (c) and the electron cross-field current (d). The thruster operating conditions: the discharge voltage of 250 V and the xenon flow rate of 4 sccm. In each thruster case, the magnetic field is unchanged.

a)

b)

Fig. 6. Plasma plume from the annular Hall thruster in the self-sustained and non-self-sustained regimes. The emissive probe is used to measure the plasma potential at the channel exit. A movable Langmuir probe is used to measure plasma properties in the near-field plume.

a)



b)

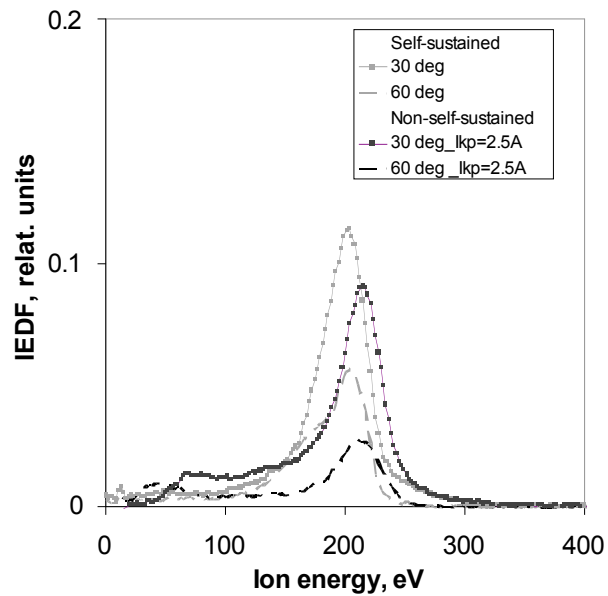


Fig. 7. Ion energy distribution function measured for the annular thruster in the far-field plume (70 cm from the thruster) at different angular positions of the retarding potential analyze: a) centerline and b) 30° and 60° with the respect to the centerline. In both self-sustained and non-self-sustained regimes the thruster was operated with the same operating parameters (250V and 3.4 sccm) and the same magnetic field.

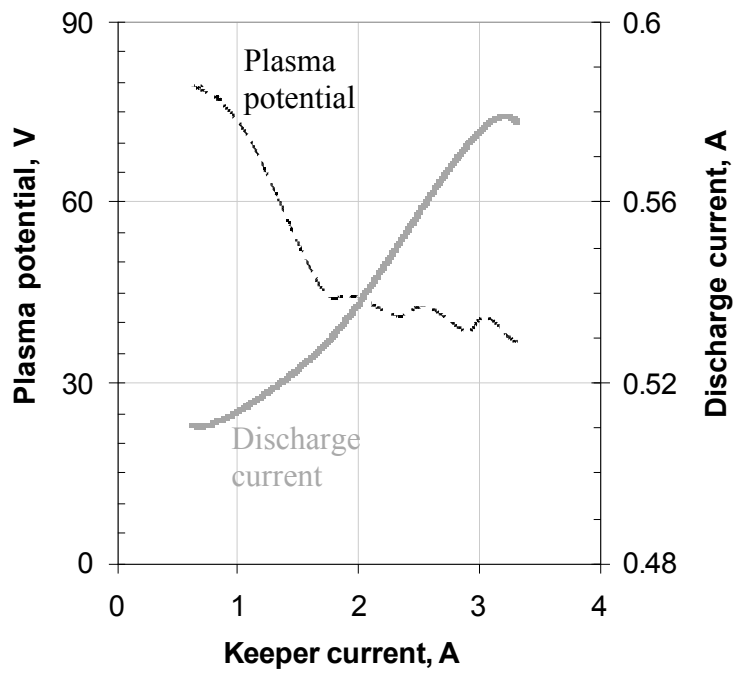
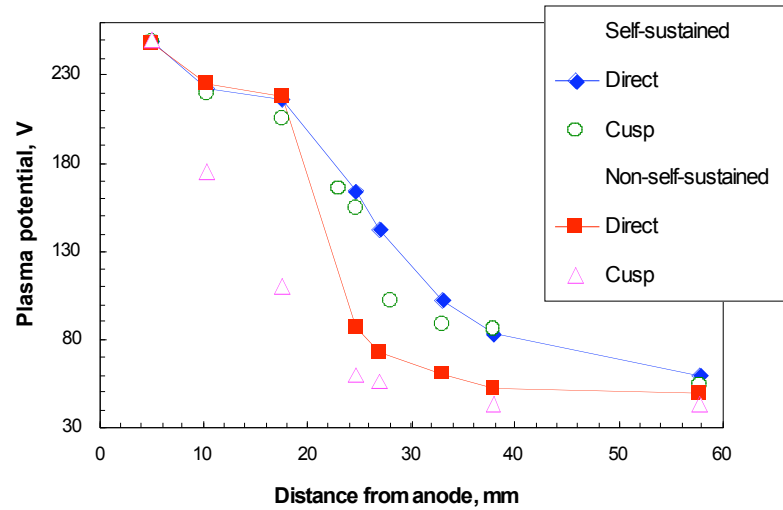


Fig. 8. Results of measurements in the annular HT. The effect of the cathode electron emission (keeper current) on the discharge current and the plasma potential (with respect to the cathode) at the channel exit.

a)



b)

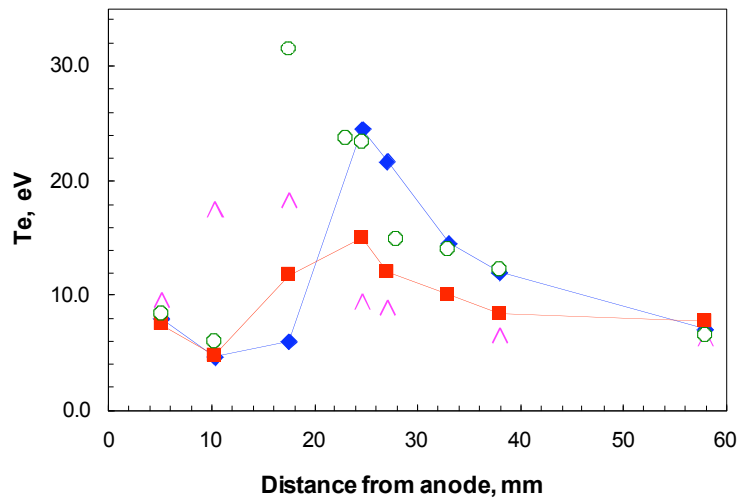
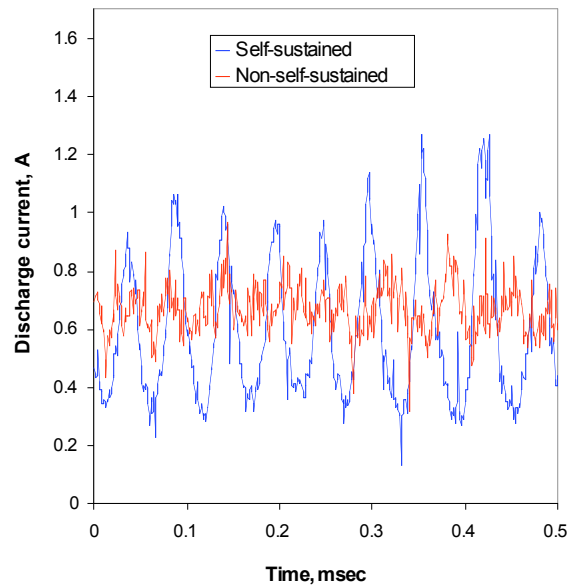


Fig. 9. Results of the plasma probe measurement in the CHT for the direct and cusp magnetic field configurations. The thruster was operated in the self-sustained (keeper current = 0 A) and non-self-sustained (keeper current = 2.5 A) regimes at the discharge voltage of 250 V and the xenon gas flow rate of 4 sccm. The plasma potential (a) and the electron temperature (b) were deduced using standard procedures for a biased Langmuir probe.<sup>24</sup> The annular part of the channel is  $0 < z$  (mm)  $< 6$ ; the cylindrical part of the channel is  $6 < z$  (mm)  $< 22$ .

a)



b)

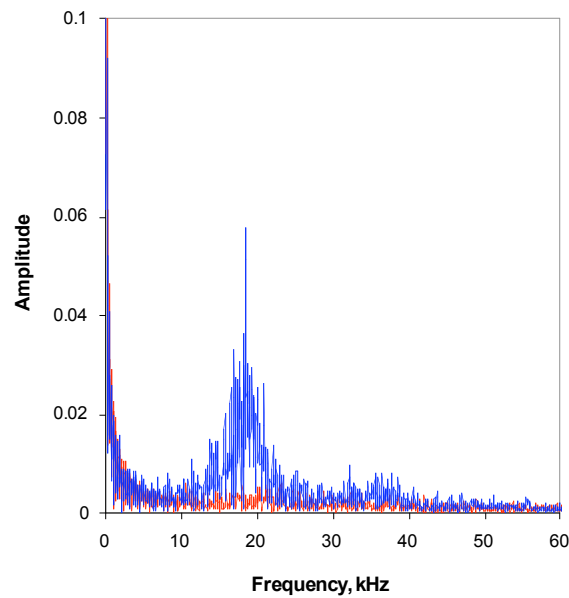
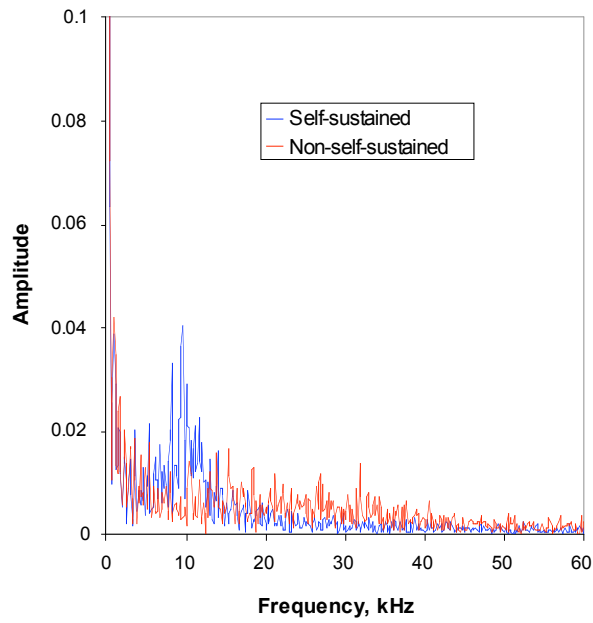


Fig. 10. The oscilloscope traces of the discharge current oscillations (a) and corresponding frequency spectrum (b) for self-sustained and non-self-sustained regimes of the annular HT.

a)



b)

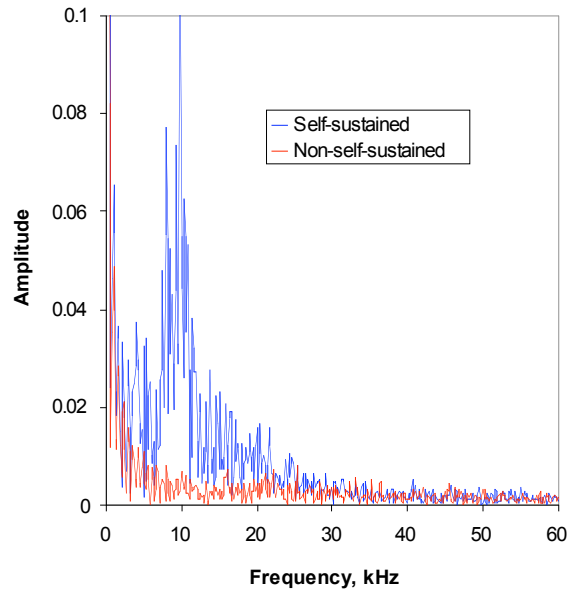


Fig. 11. Frequency spectrum measured for the self-sustained and non-self-sustained regimes of the 2.6 cm CHT operated in the direct (a) and cusp (b) magnetic field configurations.



The Princeton Plasma Physics Laboratory is operated  
by Princeton University under contract  
with the U.S. Department of Energy.

Information Services  
Princeton Plasma Physics Laboratory  
P.O. Box 451  
Princeton, NJ 08543

Phone: 609-243-2750  
Fax: 609-243-2751  
e-mail: [pppl\\_info@pppl.gov](mailto:pppl_info@pppl.gov)  
Internet Address: <http://www.pppl.gov>